Electronic Supplementary Material (ESI) for CrystEngComm.

Electronic Supplementary Information

Morphology and composition evolutions of one-dimensional $In_xAl_{1-x}N$ nanostructures induced by vapour pressure ratio

Lingyu Du, Qiang Wu,* Xiaozhu Pei, Tao Sun, Yongliang Zhang, Lijun Yang, Xizhang Wang, Zheng Hu

Key Laboratory of Mesoscopic Chemistry of MOE and Collaborative Innovation Center of Chemistry for Life Sciences, Jiangsu Provincial Laboratory for Nanotechnology, School of Chemistry and Chemical Engineering, Nanjing University, Nanjing 210023, China

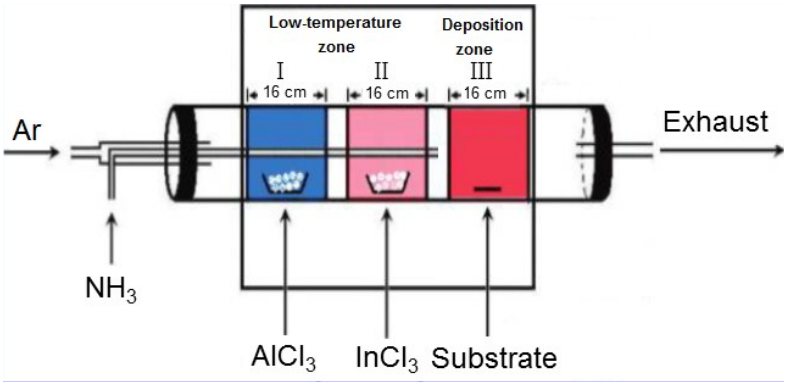

Fig. S1 Schematic illustration of the three-temperature-zone furnace.

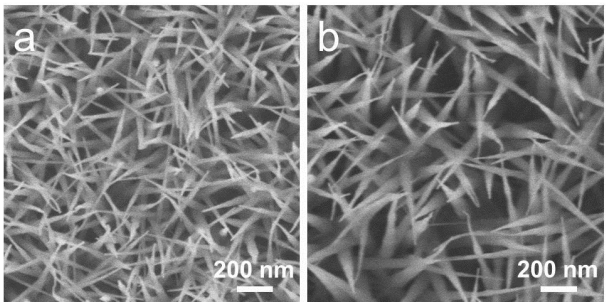

Fig. S2 SEM images of the $In_xAl_{1-x}N$ products obtained with the $InCl_3$ T_{vap} of 330 °C (a) and 460 °C (b).

It is seen the products present as quasi-aligned nanocone arrays on the Si substrate with the $InCl_3$ T_{vap} below 330 °C or above 460 °C.

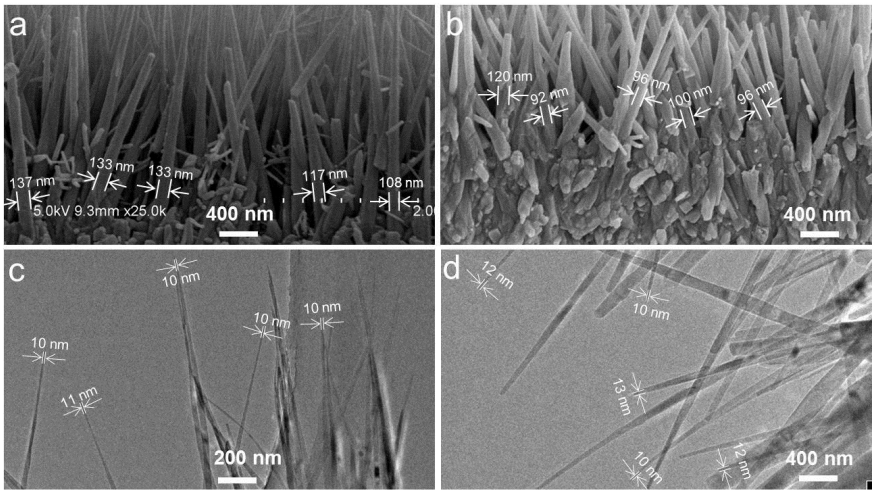

Fig. S3 High-magnification SEM images and TEM images for the $In_xAl_{1-x}N$ nanostructures with the $InCl_3$ T_{vap} of 300 °C (a,c) and 500 °C (b,d).

The SEM images in Fig. S3a,b exhibit the average diameter of the roots is ~100 nm for both of the samples. It is noticed that some nanocones with large tip diameter are also observed in the SEM images, which may come from the break of nanocones during the preparation of the SEM specimen. The TEM images in Fig. S3c,d clearly show that most of the tips have the diameter of ~10 nm.

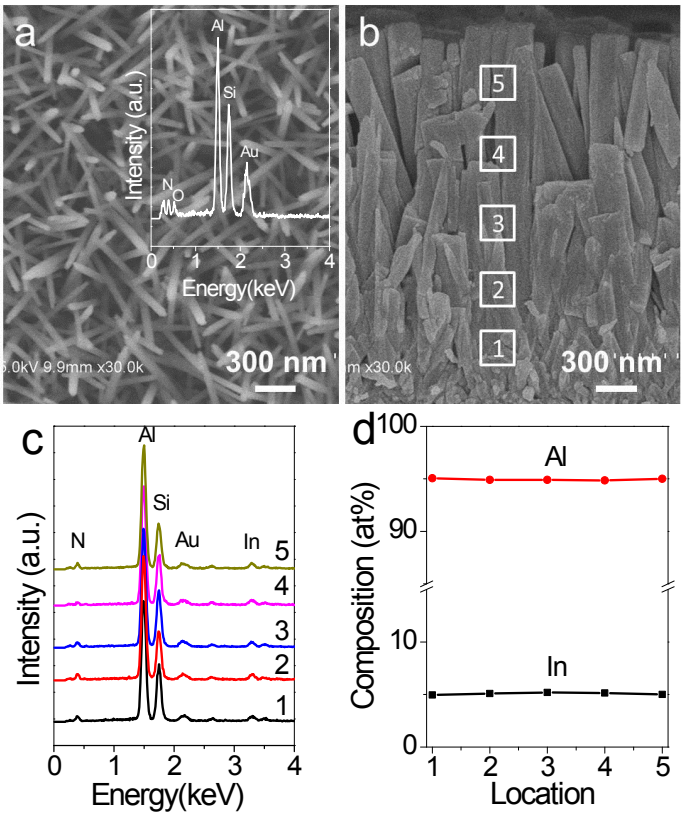

Fig. S4 SEM images of pure AlN nanocones (top-view) (a) and $In_xAl_{1-x}N$ nanocolumns (cross-section) (b). Inset in (a) is the corresponding EDS spectrum. (c) EDS spectra of the $In_xAl_{1-x}N$ nanocolumns at the five spots marked in (b). (d) element distributions of Al and In species along the axial direction of the $In_xAl_{1-x}N$ nanocolumns. Note: In EDS spectra, Si species come from the substrate and Au from the conductive layer in the SEM characterization.

The pure AlN nanocones consist of Al and N elements (O from unavoidable surface oxidation). The $In_xAl_{1-x}N$ nanocolumns consist of Al, In and N species, and the element distributions (Fig. S4d) indicate the Al and In species are uniform along the axial direction.

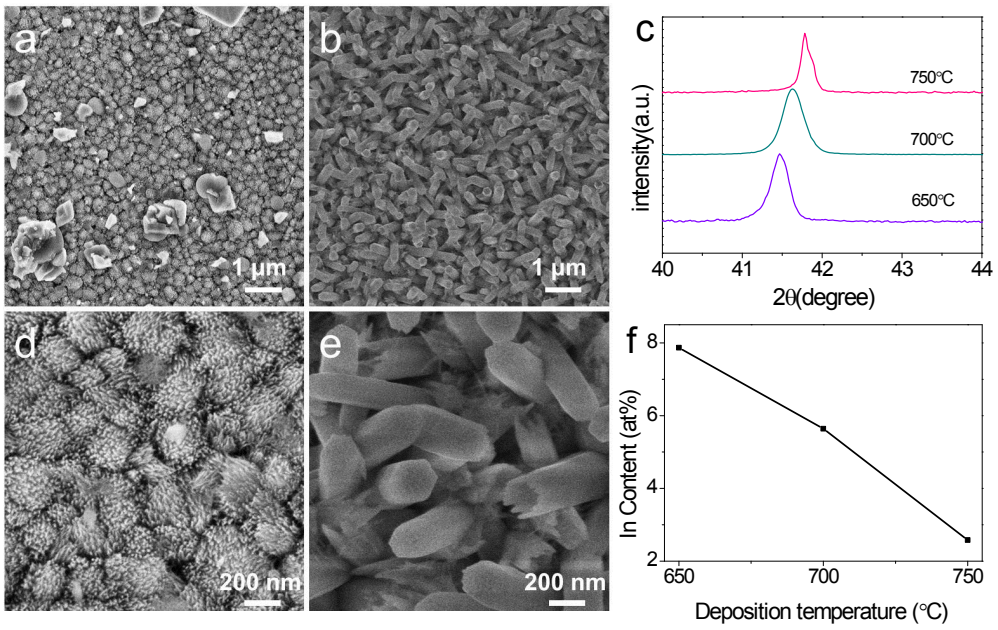

Fig. S5 Characterization results of the products obtained with the $InCl_3$ T_{vap} of 380 °C and deposition temperature of 650 °C and 700 °C. (a,d) SEM images of the product obtained at 650 °C. (b,e) SEM images of the product obtained at 750 °C. (c,f) XRD patterns and the plot of In content versus deposition temperature. For comparison, the XRD pattern and In content for the product deposited at 700 °C is also shown.

In order to study the influence of the deposition temperature on the $In_xAl_{1-x}N$ products, the CCVD growth is also performed at the deposition temperature of 650 and 750 °C while keeping the T_{vap} of $InCl_3$ at 380 °C. It is seen that the deposition temperature can affect composition of the $In_xAl_{1-x}N$ products as reflected by the XRD patterns (Fig. S5c,f). The In content can be further increased to ~8 at% at the deposition temperature of 650 °C, while decreased to ~2.5 at% at the deposition temperature of 750 °C. However, the product with higher In content is not uniform in morphology as shown in Fig. S5a, and a lot of large particles are deposited on the substrate.

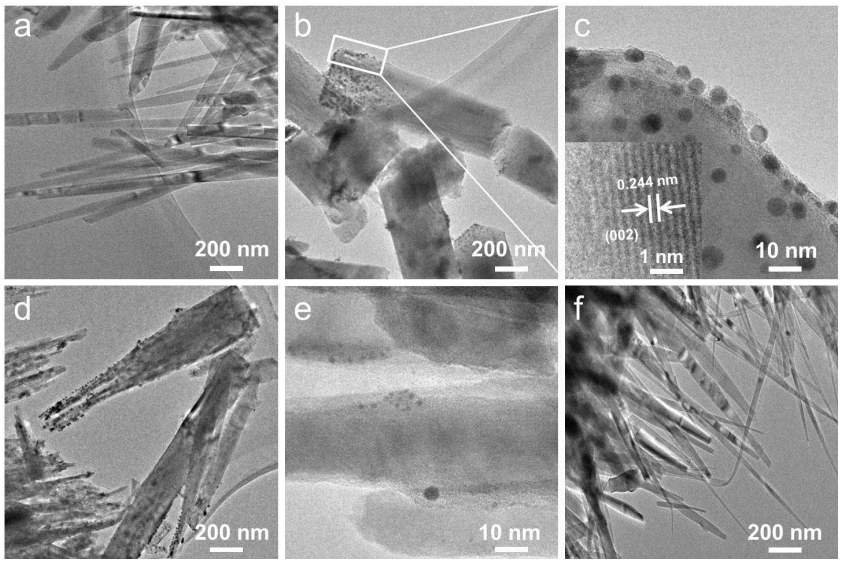

Fig. S6 TEM images of typical morphologies obtained at different T_{vap} of $InCl_3$. (a) 300 °C, (b,c) 380 °C, (d,e) 400 °C, (f) 500 °C. Note: The interplanar distance of 0.244 nm (inset of Fig. S6c) corresponds to (002) planes of metal In.

The products of 300 °C and 500 °C are nanocones with clean surfaces. At the T_{vap} of 380 °C and 400 °C, the products are nanocolumns and 'nanobrushes', respectively. It should be noticed that many nanoparticles are observed on the surface of nanocolumns and 'nanobrushes'. According to the HRTEM observation, the nanoparticles are metal In. This demonstrates the decomposition of InAlN or InN during the growth of these two products.